NASA TECHNICAL NOTE

NASA TN D-2635

FIELD-ENHANCED THERMIONIC EMISSION FROM ELECTRODES OF CESIUM ION THRUSTOR

by Joseph F. Wasserbauer

Lewis Research Center

Cleveland, Ohio

NATIONAL AERONAUTICS AND SPACE ADMINISTRATION • WASHINGTON, D. C. • JANUARY 1965

FIELD-ENHANCED THERMIONIC EMISSION FROM ELECTRODES OF CESIUM ION THRUSTOR

By Joseph F. Wasserbauer

Lewis Research Center
Cleveland, Ohio

NATIONAL AERONAUTICS AND SPACE ADMINISTRATION

For sale by the Office of Technical Services, Department of Commerce,
Washington, D.C. 20230 -- Price $1.00

FIELD-ENHANCED THERMIONIC EMISSION FROM ELECTRODES OF CESIUM ION THRUSTOR

by Joseph F. Wasserbauer

Lewis Research Center

SUMMARY

15532

An analysis is presented to estimate the drain currents due to thermionic emission from cesium-coated tantalum accelerator electrodes of an ion thrustor. The effect of electric field strength at the accelerator electrode was included in the analysis. The results of the analysis and data obtained with an experimental ion thrustor are compared. The ion thrustor was tested at current densities of 58 and 100 amperes per square meter over a range of accelerating potentials. Good agreement was obtained between the experimental data and the calculated values based on the assumptions used.

author

INTRODUCTION

Identification of the causes of accelerator electrode drain currents is desirable in order to optimize the design of electrode systems for cesium contact-ionization thrustors. Primary ion impingement on the accelerator electrodes should be kept below about 0.01 percent of the total ion current to prevent excessive erosion (ref. 1). Measured accelerator drain currents may be a sum of several effects. In addition to primary ion impingement, the possibilities include impingement of charge-exchange ions and both secondary and thermionic emission of electrons from the accelerator electrode.

Well-designed electrode geometries, obtained by both numerical and electrolytic tank analog-computer methods, have shown that primary ion impingement can be considerably reduced and perhaps completely eliminated. Impingement of charge-exchange ions on the accelerator electrode is more difficult to eliminate, and it may be the primary source of erosion (ref. 2). Thermionic emission of electrons can, however, be a major problem if the resulting electron current is large enough to overheat the ionizer. These currents also represent a power loss and must be charged to the power require-

ments of the thrustor system. Even if these currents are low, they can prevent accurate determination of ion impingement.

A recent analysis given in reference 3 showed that, with cesium-coated accelerator electrodes, accelerator drain currents of 4 percent of the ion-beam current are possible for cases where the neutral-cesium flux to the accelerator electrode comes directly from the ionizer. If a background gas pressure of cesium can build up between the interelectrode space, thermionic electron-emission currents as high as 40 percent of the ion-beam current can result. This analysis, however, was made without considering the effect produced by an electric field. A comprehensive treatment on the nature of accelerator drain currents, which includes the effect of the electric field, is given in reference 2.

The purpose of the present report is to calculate the effect of field-enhanced thermionic emission on the accelerator drain currents of an existing cesium-ion thrustor and to compare the results with experimental data.

SYMBOLS

E	field strength, V/m	u	lateral dimension in accelerator plane
f	ratio of neutral atoms to ions emitted	w	width of ionizer
I_A	accelerator drain current, A	Y	overall length of ionizer
J_A	accelerator electron-emission current density, A/sq m	μ	neutral-atom-arrival rate at the electrode, atoms/(sq cm)(sec)
J_I	ion-beam current density, A/sq m	ν_a	neutral-atom-emission rate from ionizer, atoms/(sq cm)(sec)
j	electron current density, A/sq m	Φ_A	total accelerating voltage, kV
L	accelerating length, mm	Φ_{net}	net voltage, kV
T	surface temperature, ^{o}K	φ	metal surface work function, eV

PERFORMANCE OF EXPERIMENTAL THRUSTOR

The performance of the experimental thrustor used in this investigation is reported in reference 4. The ion thrustor is presented in figure 1. The accelerator and focusing electrodes were fabricated from tantalum; the ionizer box was fabricated from sheet tungsten. The thrustor configuration has an accelerating length of 2.0 millimeters. A

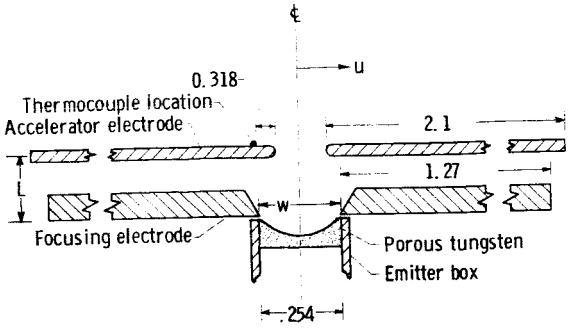

(a) Schematic cross-sectional view.

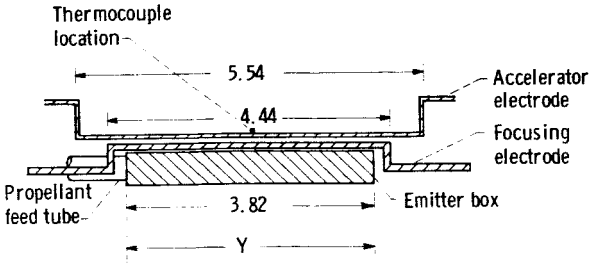

(b) Schematic side view.

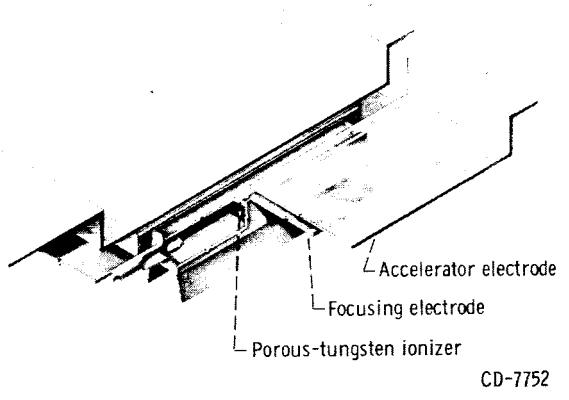

(c) Cutaway drawing.

Figure 1. - Ion thrustor. (Dimensions are in centimeters.)

thermocouple was installed on the accelerator electrode, as indicated in figure 1, to monitor the electrode temperature during thrustor operation.

The experimental thrustor configuration was analyzed on a digital computer by using a program for solving the Poisson equation (ref. 5). Theoretical ion trajectories and equipotentials obtained from the computer program are presented in figure 2 for an accelerating length of 2.0 millimeters and a ratio of net voltage to total accelerating voltage Φ_{net}/Φ_A of 0.5. The computer program assumes that a space-charge-limited current density exists across the ionizing surface, and only positive ions exist in the ion beam. The latter assumption implies a propellant utilization efficiency of 100 percent and an absence of electrons, thermionic or otherwise, in the beam. The boundary conditions imposed on the computer program are noted in figure 2. Both potentials and contours of the ionizer, focusing electrode, and accelerating electrode were specified. The axial center plane was assumed to be a plane of symmetry, and the electric field strength normal to this plane $d\Phi/dn$ was assumed to be zero. The normal electric field strength along the bounding axial plane was also assumed to be zero. The potential was assumed to be zero at a perpendicular plane located downstream from the accelerator, as shown in figure 2. This plane was intended to represent the junction of the space-charge ion flow and the neutralized ion exhaust beam.

Results obtained from the computer program include theoretical ion trajectories, equipotentials, average values of the space-charge-limited current density for a given accelerating voltage, and percent of ion impingement (if any) on the accelerator electrode. The ion trajectories show that no primary ion impingement should occur. Theo-

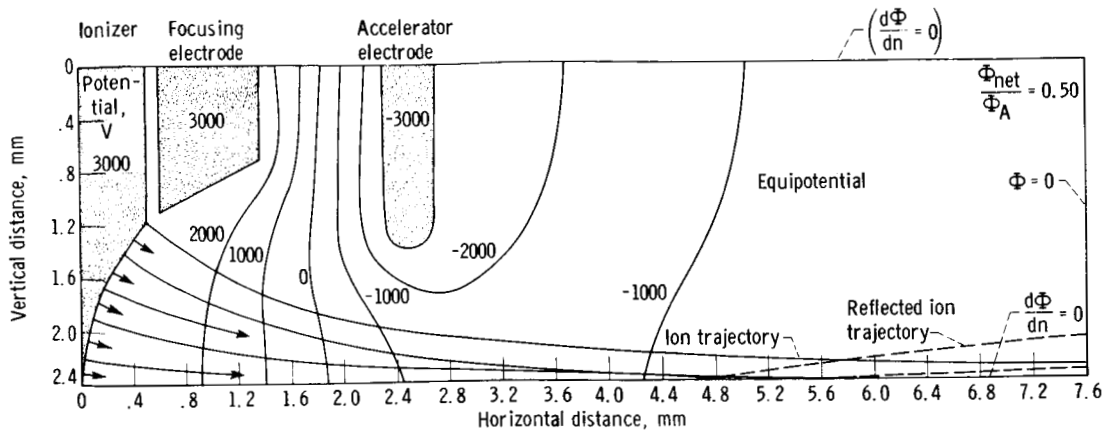

Figure 2. - Theoretical ion trajectories and equipotentials. Accelerating length, 2.0 millimeters.

retical ion trajectories for voltage ratios other than 0.5 (not presented) also indicate that no impingement of primary ions should occur.

The experimental variation of the ionizer current density as a function of total accelerating voltage is shown in figure 3. The experimentally obtained space-charge-limited line is the same as that reported in reference 4. The thrustor was tested at 58 and 100 amperes per square meter to check the field-enhanced thermionic electron emission of the accelerator electrodes for at least two ionizer current densities.

METHOD OF ANALYSIS

Although the results of the computer program showed that no primary ion impingement should occur, experimental accelerator drain currents as high as 13 and 26 percent of the beam current were recorded for beam currents of 58 and 100 amperes per square meter, respectively. As noted in the analysis of reference 3, cesium coating or adsorption on the accelerator electrodes resulting from direct impingement of neutral cesium atoms from the ionizer (distributed arrival rate) might cause accelerator drain currents as high as 4 percent of the ion beam current. This analysis does not consider the additional effects of an electric field. When the accelerator electrode is immersed in an electric field, the resulting drain current should be increased, the amount depending on the magnitude of the electric field strength at the electrode surface. A relation

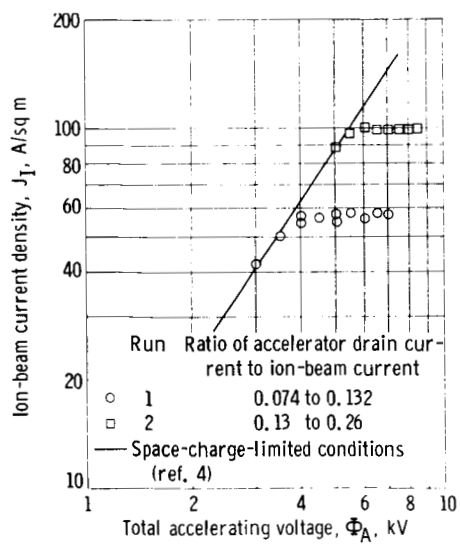

Figure 3. - Ionizer current density at various accelerating voltages. Accelerating length, 2.0 millimeters.

giving the magnitude of the current density obtained from this type of mechanism is given by the Schottky equation:

$$j = 1.2\times10^{6}\, T^{2} \exp\left(-1.16\times10^{4}\,\frac{\varphi}{T} + 0.441\,\frac{E^{1/2}}{T}\right) \qquad \frac{A}{\text{sq m}} \tag{1}$$

Equation (1) shows that the presence of an electric field will increase the thermionic electron emission from the accelerator electrodes.

For refractory metals, adsorption of cesium atoms on the metal surface can lower the work function considerably. For example, the work function of tantalum can be lowered from 4.19 to 1.4 electron volts with the adsorption of cesium. The surface work function resulting from cesium adsorption on the electrode surface will be termed the effective surface work function.

Exact determination of that portion of the accelerator drain current due to charge-exchange ions was not included in this investigation. Previous calculations (ref. 4) for this thrustor configuration showed that the ratio of charge-exchange current to ion-beam current was of the order of 10^{-3} at beam current densities of about 100 amperes per square meter. Although the charge-exchange current is small, accelerator electrode life can be seriously affected, as shown in reference 2.

The following method was used herein to estimate the magnitude of the accelerator electrode drain current due to field-enhanced thermionic emission. The arrival rate of neutral cesium atoms at the accelerator electrode is first determined. Then the effective surface work function is obtained by a technique described in reference 6. The only parameter remaining to be evaluated in equation (1) is the electric field strength at the accelerator electrode for a particular total accelerating potential. For complicated thrustor geometries, the field strengths can be obtained from computer programs such as that outlined in reference 5. When these values are substituted into equation (1) and the result is multiplied by the emissive area of the accelerator, the accelerator drain current due to field-enhanced thermionic emission is determined.

DETERMINATION OF REQUIRED PARAMETERS

Neutral-Atom-Arrival Rate

The neutral-atom efflux from a porous-tungsten ionizer is affected by several factors. The current density at which the ionizer is operated and the condition of the ionizing surface are of primary importance. Experimental data on neutral emission for commercial ionizers are reported in reference 7 and for convenience are reproduced in

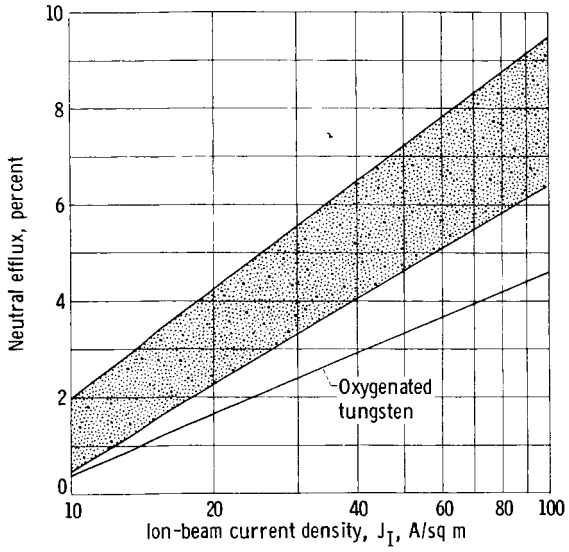

Figure 4. - Neutral flux of cesium atoms from porous tungsten at various current densities. (Data from ref. 7.)

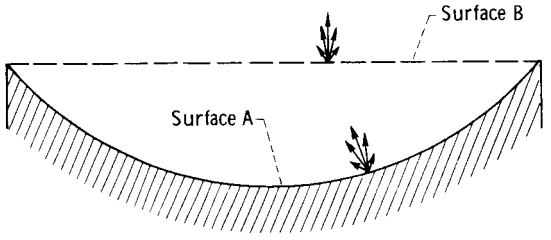

Figure 5. - Cross-sectional drawing of experimental ionizer.

figure 4. The curve used in this investigation is for oxygenated tungsten. This curve was chosen because the pressure in the vacuum facility during thrustor operation was approximately 7×10^{-6} torr.

The neutral-atom-emission rate ν_a can be written in terms of the ionizer ion-current density J_I and the ratio of neutral atoms to ions emitted f as

$$\nu_a = \left(6.25\times10^{14}\right)(f)\left(J_I\right) \quad \text{atoms/(sq cm)(sec)} \tag{2}$$

where J_I is in amperes per square meter.

In this investigation the ionizing surface was cylindrically concave. To simplify the calculations the source of neutrals was considered to be that from a flat surface. Consider the cross section of the experimental ionizer shown in figure 5. The neutrals effusing through surface A will most probably have a cosine distribution. The neutral efflux through the imaginary surface B will be the same as that from surface A, with the exception of those neutrals that can possibly strike an opposing ionizer surface (because of the cosine distribution at surface A).

The neutral-atom-arrival rate μ at the plane of the accelerator electrode is related to the neutral efflux ν_a by equation (16) of reference 3:

$$\left(\frac{\mu}{\nu_a}\right)_{u,\,Y=\infty} = \frac{1}{2}\left[\frac{1-\frac{2u}{w}}{\sqrt{4\left(\frac{L}{w}\right)^2+\left(1-\frac{2u}{w}\right)^2}}+\frac{1+\frac{2u}{w}}{\sqrt{4\left(\frac{L}{w}\right)^2+\left(1+\frac{2u}{w}\right)^2}}\right] \tag{3}$$

where u, L, and w are defined in figure 1(a). Equation (3) was obtained for a rectangular ionizing surface in the limit as the ratio of length to width approaches infinity. This equation is a good approximation for thrustors with length-width ratios greater than 10, such as the experimental thrustor of this study. The resulting variation of arrival

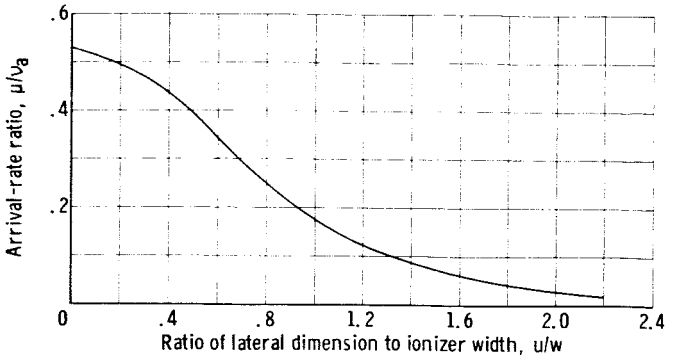

Figure 6. - Variation of arrival-rate ratio in u-direction. Accelerator spacing ratio, 0.80; overall ionizer length, ∞.

rate at the plane of the accelerator electrode in the u-direction (perpendicular to the beam) for an accelerator spacing ratio L/w of 0.80 (the experimental value) is presented in figure 6.

Electrode Temperature

A thermocouple was installed 0.318 centimeter away from the edge of the aperture at the midpoint of the accelerator electrode (see fig. 1, p. 3). During the investigation, the accelerator electrode temperature was held at 753° K by maintaining the average ionizer temperature at 1455° K. The calculations for the field-enhanced thermionic emission are based on this accelerator electrode temperature.

Electric Field Strength

The electric field strength for the experimental thrustor was obtained from the computer program (ref. 5). The equipotentials were plotted for a voltage ratio Φ_{net}/Φ_A of 0.5 as in figure 2. Shown in figure 7 is the electric field strength along the flat surface of the accelerator electrode for a range of accelerating potentials. The field strength was obtained by first cross-plotting the equipotential lines as a function of the distance to the accelerator electrode and then calculating the slope of the curves at the electrode surface. Only the field strengths at the accelerator electrode surface facing the ionizer were considered. Preliminary calculations indicated that the difference in field strength between the flat surface and the curved edge of the accelerator electrode resulted in a negligible change in the total electron-emission current density. Consequently, the flat surface values were used in the calculations.

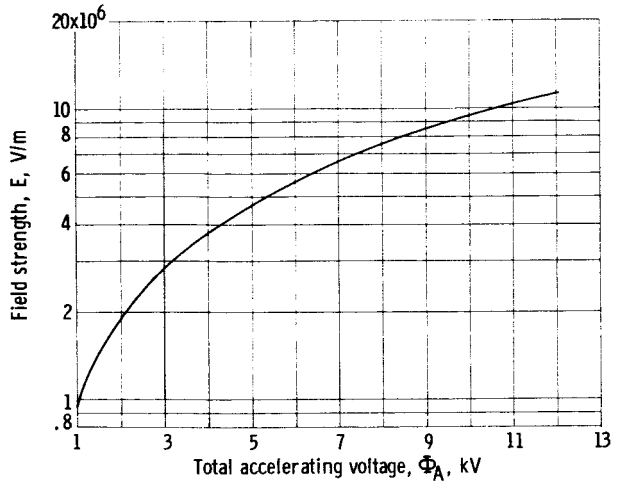

Figure 7. - Field strength as function of total accelerating voltage along flat surface from computer program.

Effective Work Function

Electron emission characteristics from

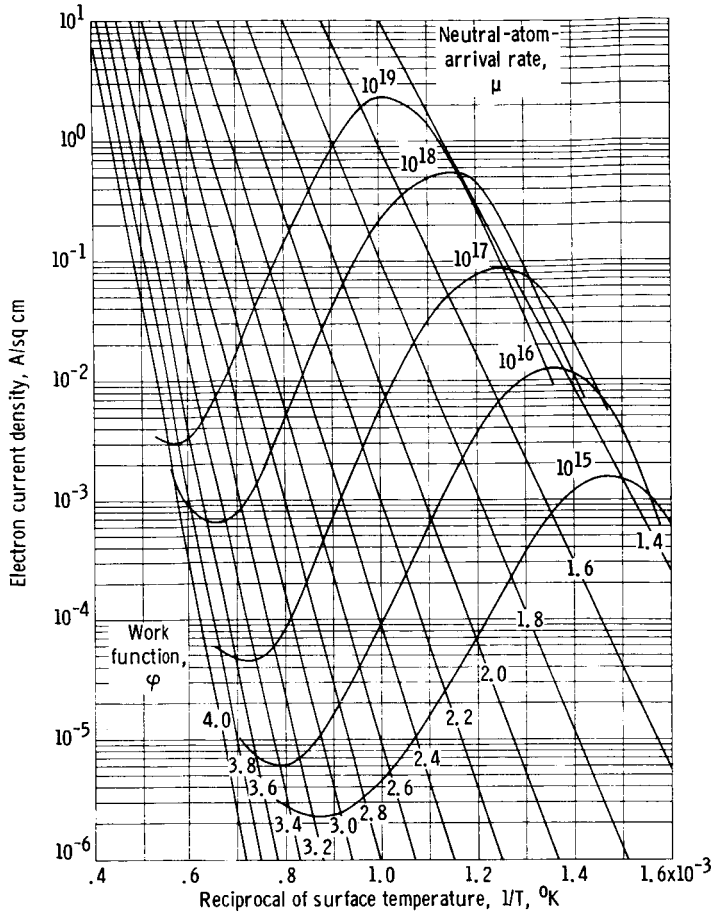

Figure 8. - Experimental electron emission from tantalum metal in cesium atmosphere. (Data from ref. 9.)

refractory metals in a cesium atmosphere result in curves of the type presented in reference 8 for a cesium-tungsten system. These curves are the S-shaped curves of the electron emission rate as a function of the base metal temperature for various cesium pressures or cesium equilibrium temperatures. The electron emission characteristics from a tantalum-cesium system at various cesium equilibrium temperatures are presented in figure 8, which is based on the experimental data reported in reference 9.

The following physical behavior generates this type of curve. At the high electrode temperatures (low 1/T) little or no cesium is adsorbed on the electrode surface, and the electron emission is that of a clean metal surface (Richardson-Dushman equation). As the electrode temperature is lowered, the progressive adsorption of cesium on the surface lowers the surface work function, which more than compensates for the decreasing electrode temperature and results in an increased electron emission until a maximum is reached. As the electrode temperature is further decreased, the surface becomes covered with cesium so that the thermionic emission curve becomes a curve for cesium alone.

The effective work function of the electrode can be obtained directly by a technique described in reference 6, which involves plotting points of intersection of constant-work-function lines of figure 8 with the experimental S-curves. The results are shown in figure 9. The process can be easily reversed, and additional S-curves for any desired value of μ can be obtained.

PROCEDURE

The following procedure was used to estimate the accelerator drain currents result-

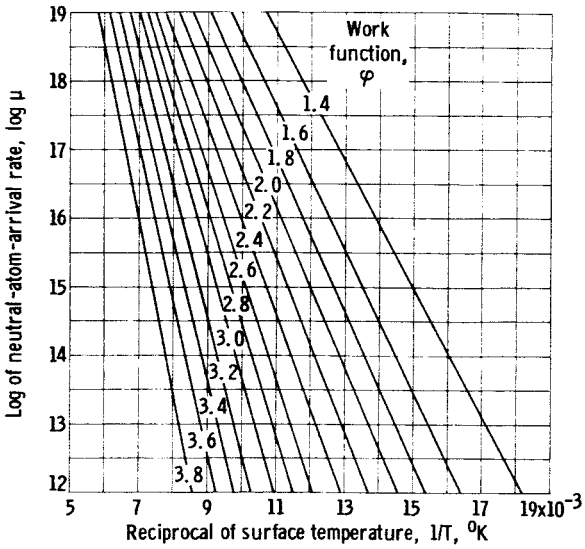

Figure 9. - Equilibrium evaporation (arrival) rate of cesium on tantalum at constant work function plotted against reciprocal of surface temperature.

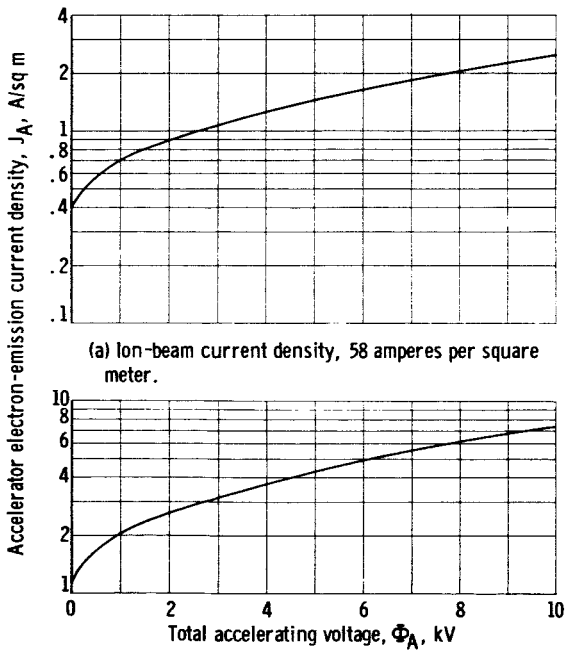

(a) Ion-beam current density, 58 amperes per square meter.

(b) Ion-beam current density, 100 amperes per square meter.

Figure 10. - Electron current density from accelerator electrode.

ing from field-enhanced thermionic emission. The neutral-cesium-emission rate from the ionizer at a particular ionizer current density was determined by using figure 4 and equation (2). The variation of arrival rate of the neutral cesium atoms across the width of the accelerator surface was then obtained from figure 6. The arrival rate was determined for segments of size $\Delta(u/w) = 0.10$, from $u/w = 0.4$ to 2.0. The calculations did not extend beyond $u/w = 2.0$ because the focusing electrode prevents direct neutral-atom impingement beyond this point (fig. 1, p. 3). (This analysis does not take into account neutral atoms that reflect or reevaporate between the accelerator and the focusing electrodes.)

The effective work function of each segment was obtained from figure 7 by knowing the electrode surface temperature and the estimated neutral-atom-arrival rates. The effective work functions from all the segments were arithmetically averaged to obtain the effective work function of the electrode surface. Since the total increment in the work function from $u/w = 0.4$ to 2.0 was only 0.23 electron volts, this averaging process is sufficiently accurate.

The effective work function of the accelerator electrode was calculated in this manner for ionizer current densities of 58 and 100 amperes per square meter. Use of equation (1) with the electric field data of figure 7 then gave the expected field-enhanced emission current density as a function of the total accelerating potential for the ionizer current densities considered. Results of these estimates are plotted in figure 10.

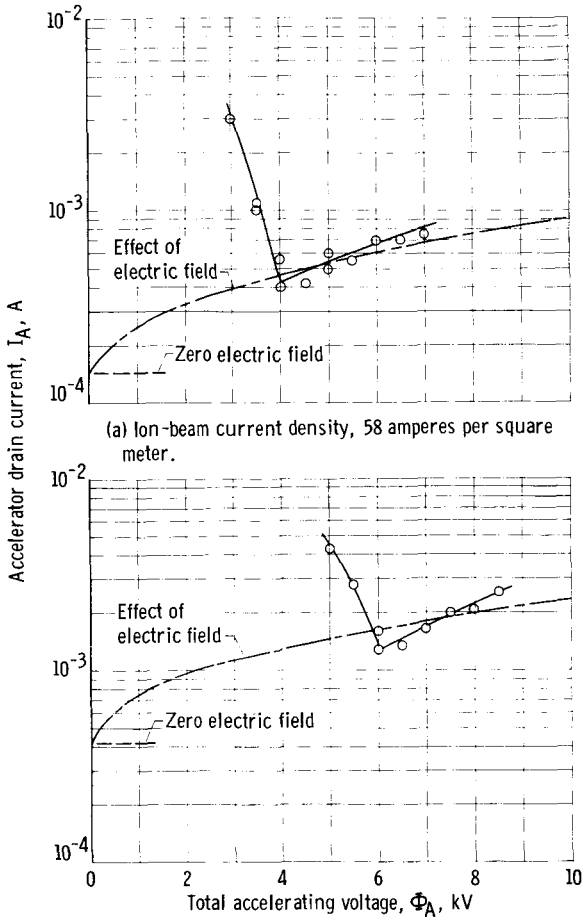

(a) Ion-beam current density, 58 amperes per square meter.

(b) Ion-beam current density, 100 amperes per square meter.

Figure 11. - Comparison of experimental and calculated accelerator drain currents.

The remaining parameter to be determined is the effective emission area of the accelerator electrode. For this purpose, the length of the accelerator electrode was taken to be 4.44 centimeters, the length of the focusing electrode (fig. 1, p. 3), because the electric field strength is probably constant over this length and the arrival-rate distribution is relatively flat over about 80 percent of the ionizer length (ref. 3). The width of the accelerator electrode was taken from the inner edge (u/w = 0.4) to the limit of direct arrival of neutral atoms from the emitter (u/w = 2.0). With this area, the total field-enhanced thermionic emission from the accelerator electrode was calculated for the two ionizer current densities.

RESULTS AND DISCUSSION

Results of the calculations are compared in figure 11 with the experimental accelerator drain currents. The dashed curve represents the results of the analysis showing the effect of electric field and also the value that would be obtained for zero electric field. The field-enhanced values of the present analysis are equal to the distributed-arrival-rate values of reference 3 multiplied by the factor

$$\exp\left(0.441\,\frac{E^{1/2}}{T}\right)$$

The portions of the experimental data in figure 11 that decrease with increasing accelerating potential were obtained with the ion thrustor operating space-charge limited but with excess propellant flow. The measured accelerator drain currents in this range may be largely due to the increased electron emission that results from the increased neutral-atom-arrival rate at the accelerator electrode. This increase in neutral-atom-arrival rate results from a higher neutral efflux of cesium atoms at these space-charge-

limited conditions. Also charge-exchange impingement would be expected to increase because of the greater number of neutral atoms and the increased value of cross section for reaction at these lower accelerating potentials (ref. 10). The portions of the data that increase with increasing accelerator potential are for the ionizer operating at ion-emission-limited conditions, the region of interest in this investigation. At ion-emission-limited conditions, the accelerator drain current should be mostly electron emission.

It was shown earlier that the ratio of accelerator drain current to ion-beam current varied from 0.074 to 0.132 at ion-beam densities of 58 amperes per square meter and from 0.13 to 0.26 at ion-beam densities of 100 amperes per square meter when the thrustor was operating at emission-limited conditions.

The data of figure 11 indicate that good agreement was obtained between the calculated and the experimental results. All data presented in figure 11 are for a ratio of net voltage to total accelerating voltage of 0.5.

Although the field-enhanced thermionic electron emission can be classed as a "nuisance" current, it does represent a power loss to the thrustor system. Fabricating porous-tungsten ionizers with lower neutral emissions should reduce these "nuisance" currents and improve the power efficiency of the thrustor system. Reduction of the neutral emission would also reduce the charge-exchange impingement and result in longer electrode life.

CONCLUSIONS

The effect of the electric field strength on the thermionic electron emission from cesium-coated accelerator electrodes of ion thrustors was considered, and the results were compared with the data obtained from an experimental cesium thrustor.

Good agreement was obtained between the experimental and the calculated values based on the assumptions used. Reduction of the neutral emission from the porous-tungsten ionizers would reduce this thermionic electron emission.

Lewis Research Center,
National Aeronautics and Space Administration,
Cleveland, Ohio, November 24, 1964.

REFERENCES

1. Brewer, G. R.; Currie, M. R.; and Knechtli, R. C.: Ionic and Plasma Propulsion for Space Vehicles. Proc. IRE., vol. 49, no. 12, Dec. 1961, pp. 1789-1821.

2. Brewer, G. R.: On the Nature of Leakage Currents in Cesium Contact Ion Engines. Res. Rep. 281, Hughes Res. Lab., Aug. 1963.

3. Reynolds, Thaine W.; and Richley, Edward A.: Thermionic Emission from Cesium-Coated Electrostatic Ion-Thrustor Electrodes. NASA TN D-1879, 1963.

4. Wasserbauer, Joseph F.: Experimental Performance of a High-Current-Density Cylindrical Concave Porous Tungsten Emitter for Ion Thrustors. Paper 63029-637 AIAA, 1963.

5. Hamza, Vladimir; and Richley, Edward A.: Numerical Solution of Two-Dimensional Poisson Equation: Theory and Application to Electrostatic-Ion-Engine Analysis. NASA TN D-1323, 1962.

6. Aarmodt, R. L.; Brown, L. J.; and Nichols, B. D.: Thermionic Emission from Molybdenum in Vapors of Cesium and Cesium Fluoride. Jour. Appl. Phys., vol. 33, no. 6, June 1962, pp. 2080-2085.

7. Husmann, O. K.: Experimental Evaluation of Porous Materials for Surface Ionization of Cesium and Potassium. Preprint 2359-62, ARS, 1962.

8. Taylor, John B.; and Langmuir, Irving: The Evaporation of Atoms, Ions, and Electrons from Caesium Films on Tungsten. Phy. Rev., vol. 44, no. 6, Sept. 15, 1933, pp. 423-458.

9. Gibbons, M. D.: Experimental Studies of the Emission and Discharge Characteristics of the Ta-Cs System. Advanced Energy Conversion, vol. 2, 1962, pp. 527-543.

10. Speiser, R. C.; and Vernon, R. H.: Cesium Ion-Atom Charge Exchange Scattering. Paper 2068-61, ARS, 1961.